PRIFYSGOL
BANGOR
UNIVERSITY

Robust Control for an Active Suspension System via Continuous Sliding-Mode Controllers

Ovalle, Luis; Rios, Hector; Ahmed, Hafiz

Engineering Science and Technology, an International Journal

Cyswllt i'r cyhoeddiad / Link to publication

16. Mar. 2022

Full Length Article

Robust Control for an Active Suspension System via Continuous Sliding-Mode Controllers

Luis Ovalle [a], Héctor Ríos [b,c,*], Hafiz Ahmed [d]

[a] Universidad Nacional Autónoma de México, Facultad de Ingeniería, CDMX, C.P. 04510, Mexico
[b] Tecnológico Nacional de México/I.T. La Laguna, División de Estudios de Posgrado e Investigación, Blvd. Revolución y Cuauhtémoc S/N, Torreón, Coahuila C.P. 27000, Mexico
[c] Cátedras CONACYT, Ciudad de México, Av.Insurgentes Sur 1582, C.P. 03940, Mexico
[d] Nuclear Futures Institute, Bangor University, Dean Street, Bangor LU57 1UT, United Kingdom

ARTICLE INFO

ABSTRACT

In this paper, a simple control methodology is proposed to stabilize the position of the sprung mass of the quarter car system. The simplicity of the structure of the proposal facilitates the application in real systems. Such methodology allows five different continuous sliding-mode controllers to be selected by means of two similar designs to mitigate the *chattering* effect. These robust controllers ensure the exponential stability of the sprung mass of a quarter car system in the presence of some class of non-vanishing disturbances. The closed-loop stability is guaranteed by means of a Lyapunov function approach and Input-to-State Stability properties. Some simulations and comparisons show the effectiveness of the proposed control schemes compared to a classic linear approach. Additionally, some experimental results show the effectiveness of the proposed controllers in the Quanser Active Suspension System.

1. Introduction

Instrumentation and control plays a vital role in automotive systems. Recent advances in control of automotive systems such as autonomous vehicles [1], traction system [2], active steering [3] and anti-lock brake systems [4] have shown that advanced control techniques can significantly improve the safety, performance and comfort of automotive systems.

Comfort is very important in passenger vehicle. Suspension system [5,6] plays an important role in proving comfort to passengers. In order to provide a higher level of comfort, a suspension system should make the movement associated with the body of the car independent from any irregularities on the terrain. This is usually managed by a *passive* suspension which performs this task by means of springs and dampers. These mechanical elements cannot adapt themselves to differences in the terrain and offer a predetermined response.

To overcome the limitation of passive suspension, active suspension has been introduced in the literature. The introduction of *active* suspension systems, *i.e.,* those that can exert a force which changes the suspension characteristics, can provide a more comfortable driving experience by injecting or subtracting damping to the system in such a way that the suspension better adapts to the terrain [7]. The main problem related to the control design for an active suspension system is its under-actuated nature, *i.e.,* it has more degrees of freedom than actuators. It is a well-known fact that it is more challenging to control under-actuated systems unlike fully-actuated ones. Nonetheless, a number of techniques have been used to control underactuated systems, *e.g.,* H_∞, model predictive control, Lyapunov-based approaches, neural controllers, *etc.* In a real world application, the parameters of a car are expected to vary, *e.g.,* the mass of the car may vary hundreds of kilograms if it is ridden by one or four people. Thus, the need to design robust controllers in automotive applications is evident. Furthermore, the effect of nonidealities in the model such as actuator deadzones and unmodeled dynamics make the need for robust controllers even more dire [8,9].

Sliding-modes controllers are known for their outstanding robust performance [10], being insensible to some kind of perturbations. However, the main drawback is the so-called *chattering* phenomena, *i.e.,* very high frequency oscillations, which appear due to the discontinuous nature of the control signals. The alleviation of this phenomena by means of approximations for the discontinuous signals has been studied [11]. However, in such solutions, the robust performance is compromised.

* Corresponding author at: Tecnológico Nacional de México/I.T. La Laguna, División de Estudios de Posgrado e Investigación, Blvd.Revolución y Cuauhtémoc S/N, Torreón, Coahuila C.P. 27000, Mexico.
  E-mail address: hriosb@correo.itlalaguna.edu.mx (H. Ríos).

Another approach to mitigate the effects of *chattering* are continuous sliding-modes controllers (see, *e.g.,* [12–15]). These controllers provide a continuous control signal, theoretically eliminating the *chattering* effect. The main idea behind the continuity of such approaches is to integrate the discontinuous components of the control signal. Nevertheless, the continuity of the control signal implies a reduction on the class of disturbances these controllers are able to deal with [10]. For instance, while a first-order sliding-mode controller is able to cope with bounded perturbations, the Super-Twisting algorithm, a *continuous* controller for systems with relative degree one, is insensible to Lipschitz continuous perturbations [10].

In the context of robust control for active suspension systems, a lot of work can be found. In [16,17], a fuzzy controller with particle swarm organization is presented. A fuzzy sliding-mode controller is introduced in [18,19] to stabilize a car. In [20], an adaptive control based on neural networks is presented. In [21], $\mathscr{H}_2$ and $\mathscr{H}_\infty$ controllers for active suspension system are proposed. An intelligent feedback linearization controller for electro–hydraulic suspension system is proposed in [22]. In [23] a quasi-sliding-mode controller is presented based on a boundary layer approach; however, the robustness of the controller is compromised. In [24], a backstepping based controller is proposed for active suspension system. A feedback linearization controller together with a linear disturbance observer is presented in [25]; the observer ensures the stability of the system in the presence of dead-zones and hysteresis on the actuator. In [26], a nonlinear controller is used to solve a double control objective, where the control scheme changes according to some signal to either stabilize the position of the car mass or the deflection of the suspension. Some applications of Lyapunov functions based controllers can also be found in [27,28].

The cited literature shows a trend to merge two or more control techniques in order to achieve an acceptable performance.This means that the computational burden to implement such schemes is higher than a controller relaying on a singe loop. In applications where the sampling time is critical and the on-board computers have a restricted power in terms of operations, such as automotive applications, the computational burden is very important. Furthermore, the application of heuristic techniques such as fuzzy controllers, neural networks and metaheuristic algorithms in conjunction with sliding-mode controllers gives a good solution of the control problem [29–31]; nonetheless this is done by means of a fairly deep understanding of the process to be controlled. This, in turn, means that a more capable workforce needs to be employed, raising the prices of product.

In contrast, due to the remarkable robustness properties of sliding-mode controllers, these approaches result in much simpler schemes from a computational point-of-view. One of the problems when designing such controllers is the need to know some kind of bound on the perturbation and/or its derivative. Nonetheless, this bound can be found through a series of simple tests. With respect to the mentioned literature, the schemes presented in [23,25] are of particular interest, since some controllers based on sliding-mode control theory are proposed. Specifically, in [23], an approximation to a sliding-mode controller is used along with a disturbance observer; in this approach it is not possible to consider the discontinuous algorithm since it is required to ensure that the disturbance term is Lipschitz continuous; thus, robustness properties of the controller are degraded. On the other hand, in [25], a feedback linearization controller is proposed. Such a scheme can be seen as a sliding-mode controller where the discontinuous term is replaced by a linear term. Thus, the stability is ensured by means of a linear disturbance observer. Both of these approaches consider the disturbance terms to be Lipschitz continuous and only achieve an ultimate bound for the position of the sprung mass.

Thus, based on the difficulties presented in the literature to stabilize the position of the sprung mass of the quarter car system, this work contributes with the following:

- A simple design procedure, which does not require external components such as disturbance observers or computationally expensive methods.
- The usage of state-of-the-art sliding-mode algorithms to control a quarter-car suspension system.
- Exact and finite-time compensation of Lipschitz continuous disturbances by means of a continuous control signal.
- The closed-loop stability guaranteed by means of Lyapunov functions and ISS properties.
- Simulation and experimental results validating the theoretical results.

The structure of the paper is given as follows: Section 2 gives some preliminaries, while Section 3 shows the problem statement. Section 4 deals with the design of the robust controllers. Section 5 shows some simulation results. Section 6 shows some experimental results and Section 7 provides some concluding remarks.

2. Preliminaries

Let $\mathbb{R}_+$ denote the set of all non-negative real numbers. For a (Lebesgue) measurable function $d : \mathbb{R}_+ \to \mathbb{R}^m$ define the norm $\|d\|_{[t_0,t_1)} = \mathrm{esssup}_{t\in[t_0,t_1)}\|d\|$, then $\|d\|_\infty = \|d\|_{[0,\infty)}$. The set with the property $\|d\|_\infty < \infty$ is denoted as $\mathscr{L}_\infty$. A continuous function $\alpha : \mathbb{R}_+ \to \mathbb{R}_+$ belongs to the class $\mathscr{K}$ if it is strictly increasing and $\alpha(0) = 0$; it belongs to class $\mathscr{K}_\infty$ if it is also unbounded; a continuous function $\beta : \mathbb{R}_+ \times \mathbb{R}_+ \to \mathbb{R}_+$ belongs to the class $\mathscr{K}\mathscr{L}$ if for each fixed $s, \beta(\cdot, s) \in \mathscr{K}$, and $\beta(r, \cdot)$ is strictly decreasing to zero for any fixed $r \in \mathbb{R}_+$.

Consider a time-dependent differential equation:

$$\frac{dx(t)}{dt} = f(t, x(t), w(t)), \, t \geqslant t_0, t_0 \in \mathbb{R}, \tag{1}$$

where $x \in \mathbb{R}^n$ represents the state vector and $w \in \mathbb{R}^q$ is an external disturbance; $f : \mathbb{R} \times \mathbb{R}^n \to \mathbb{R}^n$ is a continuous function with respect to x and piece-wise continuous with respect to t, such that $f(t, 0, 0) = 0$ for all $t \in \mathbb{R}$. The solution of the system 1, for an initial condition $x_0 \in \mathbb{R}^n$, at a time instant $t_0 \in \mathbb{R}^n$, is denoted as $x(t, t_0, x_0, w)$ and is defined on some finite time interval $[t_0, t_0 + T)$, such that $0 < T < \infty$. Let Ω be an open neighborhood of the origin in $\mathbb{R}^n$, $0 \in \Omega$ and $w \equiv 0$.

Definition 1. [32,33] *The origin of the system 1, $x = 0$, is said to be:*

1. *Uniformly Stable (US), if for any $\varepsilon > 0$, there is $\delta(\varepsilon)$ such that for any $x_0 \in \Omega$, if $\|x_0\| \leqslant \delta(\varepsilon)$, then $\|x(t, t_0, x_0, 0)\| \leqslant \varepsilon$, for all $t \geqslant t_0$ and any $t_0 \in \mathbb{R}$;*

(a) *Uniformly Exponentially Stable (UES), if it is US and exponentially convergent from Ω, i.e., for any $x_0 \in \Omega$, there exist $k, \sigma > 0$ such that $\|x(t, t_0, x_0, 0)\| \leqslant k\|x_0\|e^{-\sigma(t-t_0)}$, for all $t \geqslant t_0$ and any $t_0 \in \mathbb{R}$;*

(b) *Uniformly Finite-Time Stable (UFTS), if it is US and finite-time convergent from Ω, i.e., for any $x_0 \in \Omega$ there exist $0 \leqslant T_{x_0} < +\infty$ such that $x(t, t_0, x_0, 0) = 0$, for all $t \geqslant t_0 + T_{x_0}$ and any $t_0 \in \mathbb{R}$. The function $T_0(x_0) = \inf\{T_{x_0} \geqslant 0 : x(t, t_0, x_0) = 0 \, \forall t_0 \geqslant t_0 + T_{x_0}\}$ is called the settling-time of the system 1.*

If $\Omega = \mathbb{R}^n$, then $x = 0$ is said to be globally US (GUS), UES (GUES) or UFTS (GUFTS), respectively.

Definition 2. [32] *The system* 1 *is said to be ISS if for any $w \in \mathscr{L}_\infty$ and any $x_0 \in \mathbb{R}^n$ there exist some functions $\beta \in \mathscr{KL}$ and $\gamma \in \mathscr{K}$ such that*

$$\|x(t, t_0, x_0, w)\| \leqslant \beta(\|x_0\|, t - t_0) + \gamma(\|w\|_\infty), \ \forall t \geqslant t_0 \geqslant 0.$$

Definition 3. [34] *A Lyapunov function V is called ISS Lyapunov function for the system* 1*, if its time derivative satisfies:*

$$\dot{V}(x) \leqslant -\alpha(x), \ \forall \|x\| > \chi(\|w\|_\infty),$$

for some $\alpha, \chi \in \mathscr{K}_\infty$.

The existence of an ISS Lyapunov function for the system 1 implies that such a system is ISS with respect to w.

3. Problem Statement

Consider the nonlinear model of a quarter car system [26] (see Fig. 1).

$$\frac{d}{dt}\begin{bmatrix} x_1 \\ x_2 \\ x_3 \\ x_4 \end{bmatrix} = \begin{bmatrix} x_2 \\ -\frac{1}{m_s}(f_s + f_d - u + w(t)) \\ x_4 \\ \frac{1}{m_u}(f_s + f_d - f_t - u + w(t)) \end{bmatrix},$$

$$f_s(x_1, x_3) = k_{s1}(x_1 - x_3) + k_{s2}(x_1 - x_3)^3,$$
$$f_d(x_2, x_4) = c_1(x_2 - x_4) + c_2(x_2 - x_4)^2,$$
$$f_t(x_3, x_4, z) = k_u(x_3 - z) + c_t(x_4 - \dot{z}),$$

where m_s and m_u represent the sprung and unsprung masses, k_{s1} and k_u represent the coefficients for the linear action of the spring for the suspension and tire, k_{s2} is the nonlinear part of the spring for the suspension, c_1 and c_t are the linear damper coefficients for the sprung and unsprung masses, c_2 represents the coefficient for the nonlinear action of the suspension damper, g is the acceleration due to gravity; x_1 and x_3 represent the positions of the sprung and unsprung masses, x_2 and x_4 are the velocities of the sprung and unsprung masses, respectively. Finally, z is an external signal repre-

Fig. 1. Schematic representation of a quarter car system.

senting the bumps and potholes of the road, generally called profile of the rode; u is the control force and w represents some disturbances such as parameter uncertainties, external forces and unmodeled dynamics.

The objective of this work is to stabilize the position of the sprung mass, *i.e.*, x_1, in the presence of external disturbances and without knowledge of the road profile.

4. Robust Control Design

The control law is composed of two controllers: a nominal controller and a one of five different robust controllers, *i.e.*,

$$u = u_n + u_r.$$

Thus, consider the following nominal controller

$$u_n = f_s(x_1, x_3) + f_d(x_2, x_4). \tag{4}$$

Then, the following closed-loop system is obtained

$$\frac{d}{dt}\begin{bmatrix} x_1 \\ x_2 \\ x_3 \\ x_4 \end{bmatrix} = \begin{bmatrix} x_2 \\ -\frac{1}{m_s}(-u_r + w(t)) \\ x_4 \\ \frac{1}{m_u}(-f_t - u_r + w(t)) \end{bmatrix}. \tag{5}$$

Thus, the problem has now become to design u_r to ensure that x_1 goes to zero, in the presence of the disturbance term w, by means of a continuous control law while ensuring the stability of the dynamics for x_2, x_3 and x_4. For this purpose, two different approaches will be considered. The first approach is based on the Super-Twisting algorithm (STA) [35], a continuous sliding-mode controller, which can robustly stabilize a relative degree one system in the presence of Lipschitz continuous disturbances. On the other hand, the second approach is based on continuous sliding-mode controllers that can stabilize relative degree two systems also in the presence of Lipschitz continuous disturbances. Before tackling the controllers design, consider the following assumption over the disturbance term w.

Assumption 1. *There exists a constant $\eta > 0$ such that*

$$\|\frac{d}{dt}w\|_\infty \leqslant \eta. \tag{6}$$

Remark 1. Assumption 1 restricts the class of disturbances to be Lipschitz continuous. This means that the considered disturbances must be continuous in nature and, in fact, cannot grow faster than a linear function of time.

4.1. STA-Based Robust Controller for Relative Degree One

Consider the following sliding variable

$$s = c_x x_1 + m_s x_2, \tag{7}$$

where $c_x > 0$ is a design parameter. Notice that taking s to zero implies that the system will be governed by the following dynamics

$$x_2 = -\frac{c_x}{m_s}x_1, \tag{8}$$

which is a linear first-order system and its exponential stability is guaranteed for any $c_x > 0$. Then, differentiating 7 and substituting the closed-loop dynamics 5, it follows that

$$\dot{s} = c_x x_2 + u_r - w(t). \tag{9}$$

It is clear that the sliding variable has relative degree one with respect to the control input. Consider the following controller
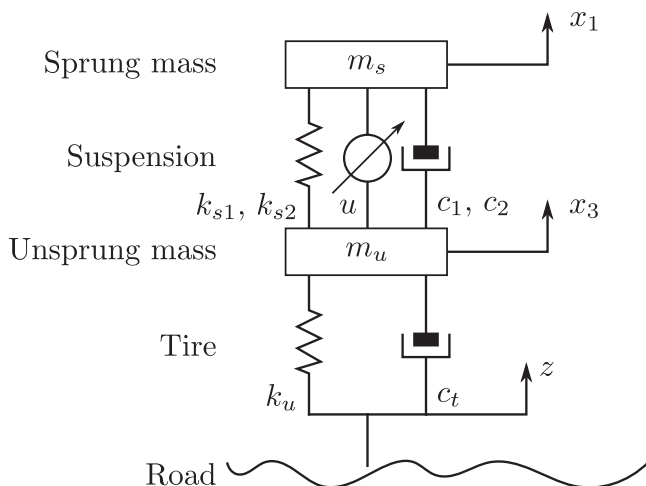
$$u_r = -c_x x_2 - k_1 \lceil s \rceil^{1/2} + v,$$
$$\dot{v} = -k_2 \lceil s \rceil^0. \tag{10}$$

Thus, the following Theorem deals with the stability of system 5.

Theorem 1. *Let the controller* 10 *be applied to system* 5, *and Assumption* 1 *hold. If the controller gains are designed as*

$$k_1 = 1.5\eta^{\frac{1}{2}}, \quad k_2 = 1.1\eta, \tag{11}$$

then, $s = 0$ is GUFTS.

Proof. By substituting the control law 10 in 9, it follows that

$$\dot{s} = c_x x_2 - \frac{k_1}{m_s} \lceil s \rceil^{1/2} + v - w(t),$$
$$\dot{v} = -k_2 \lceil s \rceil^0.$$

Define $\bar{v} := v - w$. The closed-loop dynamics can be rewritten as

$$\dot{s} = -k_1 \lceil s \rceil^{1/2} + \bar{v},$$
$$\dot{\bar{v}} = -k_2 \lceil s \rceil^0 - \dot{w}(t). \tag{12}$$

In [36], it has been proven that the function

$$V(s, \bar{v}) = \varsigma(s, \bar{v})^T P \varsigma(s, \bar{v}),$$

with $\varsigma = [\lceil s \rceil^{\frac{1}{2}}, \bar{v}]^T$ and some $0 < P = P^T \in \mathbb{R}^{2 \times 2}$, is a proper and strong Lyapunov function for system 12. Then, according to [37], if the gains are selected according to 11, $[s, \bar{v}]^T = 0$ is GUFTS.

Remark 2. Since $s = 0$ is GUFTS, it follows, from 8, that $[x_1, x_2]^T = 0$ is GUES in spite of the perturbation w.

Due to the fact that $\bar{v} = 0$ is GUFTS, v can be seen as an exact and finite-time convergent estimator of the disturbance term w.

4.2. Continuous Sliding-Mode Controllers for Relative Degree Two

Define the following function

$$s = m_s x_1.$$

Thus, from 5, it follows that

$$\frac{d}{dt} \begin{bmatrix} s \\ \dot{s} \end{bmatrix} = \begin{bmatrix} \dot{s} \\ u_r - w(t) \end{bmatrix}. \tag{13}$$

It is clear that the relative degree of s with respect to w is equal to two. Moreover, the task has been reduced to robustly stabilize the system 13. In order to design the robust controller u_r, the following algorithms are introduced:

a) Continuous Singular Terminal Sliding-Mode Controller (CSTA) [38]

$$\sigma = k_\sigma \lceil s \rceil^{2/3} + \dot{s},$$
$$u_r = -k_1 \lceil \sigma \rceil^{1/2} + \bar{v},$$
$$\dot{\bar{v}} = -k_2 \lceil \sigma \rceil^0. \tag{14}$$

One possible selection of gains is: $k_\sigma > 0$, $k_1 = 1.5\eta^{\frac{1}{2}}$, $k_2 = 1.1\eta$.

b) Continuous Nonsingular Terminal Sliding-Mode Controller (CNSTA) [14]

$$\sigma = s + k_\sigma \lceil \dot{s} \rceil^{3/2},$$
$$u_r = -k_1 \lceil \sigma \rceil^{1/3} + v,$$
$$\dot{v} = -k_2 \lceil \sigma \rceil^0. \tag{15}$$

According to [14], one possible selection of the controller gains is

$$k_\sigma = 7.7\eta^{-1/2}, \quad k_1 = 7.5\eta^{2/3}, \quad k_2 = 2\eta.$$

c) Continuous Twisting Algorithm (CTA) [13]

$$u_r = -k_1 \lceil s \rceil^{1/3} - k_2 \lceil \dot{s} \rceil^{1/2} + v$$
$$\dot{v} = -k_3 \lceil s \rceil^0 - k_4 \lceil \dot{s} \rceil^0. \tag{16}$$

In [13], it is shown that the control gains can be taken as

$$k_1 = 7\eta^{2/3}, \quad k_2 = 5\eta^{1/2}, \quad k_3 = 2.3\eta, \quad k_4 = 1.1\eta.$$

d) Discontinuous Integral Controller (DIC) [12]

$$\sigma_1 = s + k_2 \lceil \dot{s} \rceil^{3/2},$$
$$\sigma_2 = s + k_4 \lceil \dot{s} \rceil^{3/2},$$
$$u_r = -k_1 \lceil \sigma_1 \rceil^{1/3} + v$$
$$\dot{v} = -k_3 \lceil \sigma_2 \rceil^0. \tag{17}$$

In [12], the following gain selection procedure is proposed

$$k_2 > 0, \quad k_4 \in \mathbb{R}, \quad k_3 = \frac{\eta}{l}, \quad k_1 > 0,$$

for some $0 < l < 1$. Then, the following Theorem deals with the stability of the system 13 when one of the continuous controllers 14-17 is used.

Theorem 2. *Let the system* 13 *be controlled by one of the continuous controllers* 14-17; *then, $[s, \dot{s}]^T = 0$ is GUFTS.*

Remark 3. The convergence proofs of the given continuous sliding-modes controllers can be found in the corresponding references; moreover, all of them are based on Lyapunov function approaches. Furthermore, every algorithm ensures that the closed-loop system is insensible to the effect of the non-vanishing disturbance $w(t)$.

Remark 4. Notice that Theorem 2 ensures that $[s, \dot{s}] = 0$ is GUFTS. Thus, it follows that $s(t) = m_s x_1(t) = 0$ and $\dot{s}(t) = m_s x_2(t) = 0$, for all $t \geqslant T$, *i.e.*, $[x_1, x_2] = 0$ is GUFTS as well. Moreover, note that the same information is needed for the computation every controller. Thus, Theorem 2 presents a stronger theoretical result than Theorem 1.

Fig. 2 shows a representation of the closed-loop system with the proposed methodology. Note that all of the approaches use the same amount of information and that the only difference is given by the selection of the sliding-mode algorithm.

Both of the proposed methodologies, *i.e.*, the STA-based controller and all of the five continuous sliding-mode controllers, result in discontinuous closed-loop systems. Nonetheless, the control law that drives the quarter car system is continuous in nature;
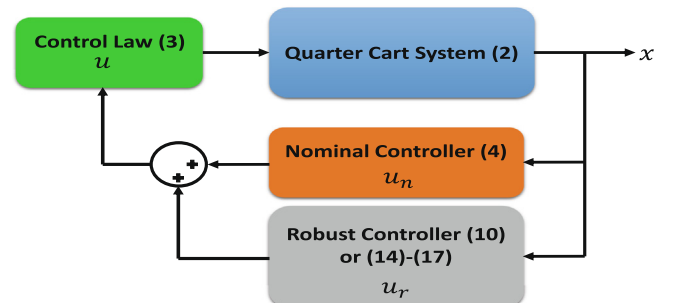
Fig. 2. Schematically representation of the proposed methodology.

thus, from a theoretical point-of-view, no *chattering* should affect the system. In terms of implementation complexity, notice that every algorithm is made up by a homogeneous nonlinear feedback and the integral of a discontinuous term to ensure the finite-time compensation of Lipschitz continuous disturbances. Therefore, none of the proposals represent a significantly higher computational burden than the others.

Furthermore, the structure of the proposed methodology and the result in [25] is similar, *i.e.*, a feedback linearization control law and a robustifying term. Furthermore, the result in [25] and the proposed methodology consider the effect of Lipschitz continuous perturbations. Then, since, in every controller considered in Section 4 the variable v can be seen as an exact and finite-time convergent approximation of the external disturbance $w(t)$, the presented methodology represents a stronger result from a theoretical point-of-view.

It is worth mentioning that, although the continuity of the control signal ensures that, theoretically speaking, no chattering effect is present, it has been proven in [39] that the presence of parasitic dynamics, such as very slow actuators, may degrade the performance of the controller. Thus, these parasitic dynamics should be considered when designing the controller in real-world applications.

4.3. Stability of the Unsprung Mass Position

Notice that, up to this point, nothing has been said about the stability of x_3 and x_4. In this sense, consider the dynamics

$$\frac{d}{dt}\begin{bmatrix} x_3 \\ x_4 \end{bmatrix} = \begin{bmatrix} x_4 \\ -\frac{1}{m_u}(f_t(x_3, x_4, z) + u_r - w(t)) \end{bmatrix}. \tag{18}$$

Define a disturbance vector $d := [z, \dot{z}, u_r - w]^T$. Then, the dynamics for x_4 can be rewritten as

$$\dot{x}_4 = \frac{1}{m_u}(-k_u x_3 - c_t x_4 + bd),$$

with $b = \frac{1}{m_u}[k_u, c_t, 1]$. Then, the following Theorem deals with the stability of system 18.

Theorem 3. *Let the control law 3, with u_n given by 4 and u_r given by either 10 or 14, be applied to system 2. Then, the dynamics 18 is ISS with respect to z and $\dot{z}$. Moreover, the system 2 is ISS with respect to z and $\dot{z}$ as well.*

Proof. Define the vector $\tilde{x} = [x_3, x_4]^T$. Thus, 18 can be described as

$$\dot{\tilde{x}} = A\tilde{x} + Bd, \tag{19}$$

where

$$A = \begin{bmatrix} 0 & 1 \\ -k_u & -c_t \end{bmatrix}, \quad B = \begin{bmatrix} 0 \\ b \end{bmatrix}.$$

Consider the following Lyapunov function candidate

$$V(\tilde{x}) = \tilde{x}^T P \tilde{x}, \tag{20}$$

where $P = P^T > 0$ is the solution to the Lyapunov equation

$$PA + A^T P = -Q,$$

for some $Q > 0$. The derivative of the Lyapunov function candidate along the trajectories of the system 19 is given by

$$\begin{aligned} \dot{V} &= \tilde{x}^T(A^T P + PA)\tilde{x} + 2\tilde{x}^T PBd, \\ &= -\tilde{x}^T Q\tilde{x} + 2\tilde{x}^T PBd, \\ &\leqslant -\lambda_{\min}(Q)\|\tilde{x}\|^2 + 2\|\tilde{x}\|\lambda_{\max}(P)\|B\|\|d\|_\infty. \end{aligned}$$

Thus, it follows that the derivative of V is bounded by

$$\begin{aligned} \dot{V}(\tilde{x}) &\leqslant -\lambda_{\min}(Q)(1-\theta)\|\tilde{x}\|^2, \\ &\forall \|\tilde{x}\| > \frac{2\lambda_{\max}(P)\|B\|}{\theta\lambda_{\min}(Q)}\|d\|_\infty, \end{aligned}$$

for any $\theta \in (0, 1)$. Therefore, 20 is an ISS Lyapunov function for system 18. Moreover, from Theorem 1, it follows that $s(t) = 0$ and $v(t) = w(t)$, for all $t \geqslant T_0$, with T_0 as the settling time of the sliding-mode controller. For the STA-based controller 10, u_r exponentially converges to w due to the presence of the term x_2 that vanishes exponentially with respect to the time. For the CSTA 14, u_r converges in a finite time to w. Thus, the only persisting disturbances acting on the system 18 are z and $\dot{z}$. Hence, system 18 is ISS with respect to $[z, \dot{z}]^T$. Moreover, this implies that the system 2 is ISS with respect to z, and $\dot{z}$ since 18 is a subsystem of 2. □

Remark 5. Notice that, although the system 2 is ISS with respect to z and $\dot{z}$, the dynamics for x_1 has been proven to be GUFTS. This means that only x_3 and x_4 are affected by z and $\dot{z}$.

5. Simulation Results

In order to test the effectiveness of the proposed schemes, a series of simulations are carried out. The parameters considered for such simulations are: $m_s = 290$[kg], $m_u = 59$[kg], $g = 9.81[m/s^2]$, $c_1 = 1385.4$[Nm^{-1} s], $c_2 = 524.28$[Nm^{-2} s^2],- $c_t = 170$[Nm^{-1} s], $k_u = 1.9 \times 10^6$[Nm^{-1}], $k_{s1} = 1.45 \times 10^4$[Nm^{-1}], $k_{s2} = 1.6 \times 10^6$[Nm^{-3}], which represent the parameters of a real vehicle.

The response of the system in a bumpy road is tested by considering the following profile.

$$z = \begin{cases} -at_1^3 + bt_1^2 + c(t); & 3.5 \leqslant t < 5, \\ at_2^3 + bt_2^2 + c(t); & 5 \leqslant t < 6.5, \\ at_3^3 - bt_3^2 + c(t); & 8.5 \leqslant t < 10, \\ -at_4^3 - bt_4^2 + c(t); & 10 \leqslant t < 11.5, \\ c(t); & \text{otherwise,} \end{cases}$$

where $c(t) = 0.002 \sin(t) + 0.002 \sin(7.5\pi t)$, $t_1 = t - 3.5$, $t_2 = t - 6.5$, $t_3 = t - 8.5$ and $t_4 = t - 11.5$.

In order to test the robustness of the schemes, a disturbance signal $w = 10 \sin(10t) + 10$ is considered. Furthermore, to taste the robustness under parameter uncertainty, it will be assumed, for control design purpose, that the parameter k_{s1} possesses 90% of its nominal value. Notice that for this disturbance signal, Assumption 1 holds with $\eta = 300$. Moreover a value of $c_x = 90$ is considered for the STA-based controller and $k_\sigma = 5$ for the CSTA.

The linear disturbance observer (LDO)-based controller, presented in [25], is considered as a point of reference in terms of the performance given by the proposed schemes.

Notice that, as stated at the end of Section 4, the proposed methodology has some common points with the result given in [25]. Thus, the next logical step is to compare their performance in a simulation setting. It is important to note that all of the approaches consider that full state information is available and the task is to reject the disturbance signal d. Furthermore, the tuning of the LDO must be done with a compromise in mind. A better precision of the approximation implies a stronger initial response which will be detrimental to the ride comfort as will be discussed latter.

In order to keep the simulation result as comprehensive as possible, the STA-based controller along with the CSTA and the LDO

are considered through the simulations. Note that only the CSTA-based robust controller is considered for the relative degree two case; such a controller was chosen due to its similarities with the STA-based controller.

Throughout the simulations the following legends are employed: OL represents the unforced open-loop response, LDO stands for the linear disturbance observer approach, STA is the STA-based controller and CSTA represents the CSTA-based approach.

Fig. 3 shows the response of the sprung mass position. The open-loop response is shown to verify the effectiveness of all of the controllers. In this figure, it is possible to see that the CSTA has the fastest transient response of all of the controllers. Additionally, the LDO has a faster transient than the STA, but its precision in the steady state is lower than the STA.

Fig. 4 displays the response for x_3, showing the boundedness of such a signal. Notice that no significant differences in the responses of the proposed controllers is present. This actually implies that a better response for the sprung mass is achieved, with respect to the open-loop response, for all of the controllers.

Fig. 5 shows the control signals. The main observation of this response is that the proposed controllers are able to better fulfill the control objective, the stabilization of x_1, with a similar level of control action as the LDO and by means of a continuous control law.

In order to assert the ride comfort, an appropriate index is needed. According to the ISO 2631 standard, the human body is more sensitive to frequency components between 4–8[Hz] for accelerations. Thus, a weighted sum of the frequency components of $\dot{x}_2$ must be computed to analyze ride comfort; this is a challenging task. However, as stated in [40], the following fifth order linear filter gives an accurate representation of such an index

$$w(p) = \frac{87.72p^4 + 1138p^3 + 11336p^2 + 5453p + 5509}{p^5 + 92.6854p^4 + 2549.83p^3 + 2569p^2 + 81057p + 79783}.$$
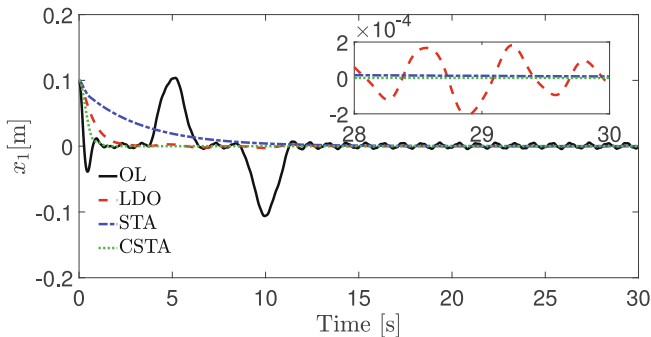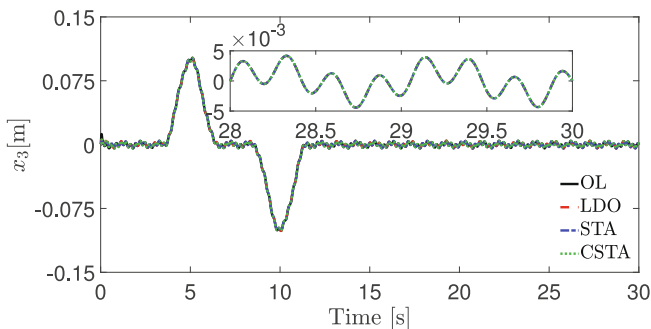

Fig. 3. Sprung mass position.

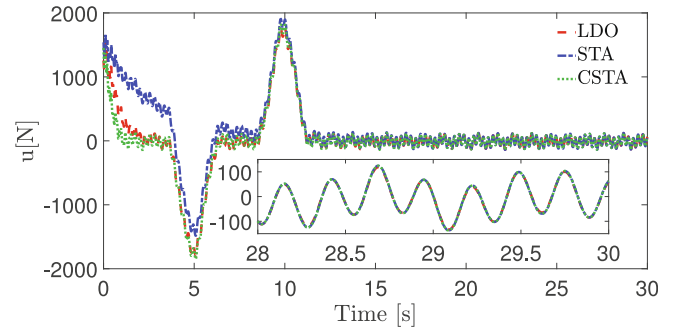**Fig. 4.** Unsprung mass position.
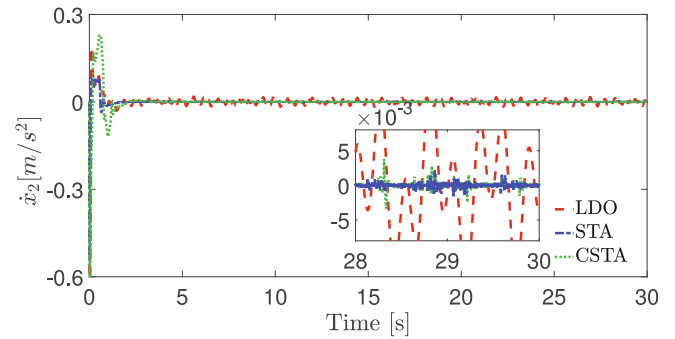

Fig. 5. Control signal.

Fig. 6. Filtered accelerations.

Fig. 6 shows the response of the filtered acceleration $\dot{x}_2$. This figure shows a superior ride quality for the proposed controllers with respect to the LDO. Notice that the precision of the LDO can be incremented with a different tuning; however, by doing so, the initial response will be heavily impacted. Thus, a compromise should be made between precision and aggressiveness of the response. This is not the case for the proposed controllers.

In order to provide a better metric for the comparison of the results, let us consider the following comparison in terms of quantitative metrics. The considered criteria for the analysis are the average of the absolute values for x_1, the filtered accelerations and u, considering a sampling time of 1 ms.

Note that, at first glance, the STA controller seems to have a worst metric in almost every case. Nonetheless, this is due to the fact that the transient response for such a variable is slower than the response for the other methodology. Then, in terms of ride comfort, this is reflected as a far superior response. Furthermore, the response for the CSTA controller achieves a vastly superior response without compromising the ride comfort with respect to the LDO controller. Thus, it can be said that the proposed methodology gives a response to both ride comfort and accuracy in the response far better than the LDO, and which of the two variables is more important will determine the selection of the controller to be implemented. Furthermore, it is important to remark that the overall accuracy of the STA controller can be improved by modifying the c_x parameter; a bigger value of c_x would imply a faster response, although ride comfort would be compromised.

6. Experimental Results

In order to show the effectiveness of the proposed controllers in a more realistic setting, some experiments were carried out in an experimental setup via the Quanser Active Suspension System, shown in Fig. 7.

The Active Suspension consists of three masses that along stainless steel shafts using linear bearings and is supported by a set of springs. The upper mass (blue) represents the vehicle body supported above the suspension, the middle mass (red) corresponds to one of the vehicle's tires, and the bottom (silver) mass simulates the road. The upper mass is connected to a high-quality DC motor through a capstan to emulate an active suspension system that can dynamically compensate for the motions introduced by the road. The lower plate is driven by a powerful DC motor connected to a lead screw and cable transmission system. For technical details about the Quanser Active Suspension System, interested readers are requested to consult the Quanser website.[1]

The parameters for the experimental platform are taken as: $m_s = 2.45$ [kg], $m_u = 1$ [kg], $g = 9.81$ [m/s^2], $c_1 = 7.5$ [Nm^{-1}s], $c_t = 5$ [Nm^{-1}s], $k_u = 900$ [Nm^{-1}], $k_{1s} = 2.5 \times 10^3$ [Nm^{-1}], while the nonlinearities are assumed to be unknown to test the robustness of the schemes.

In order to further test the robustness of the schemes, a disturbance signal $d = 0.1 \sin(10t) + 0.1$ is considered. Such a signal is added to the experimental setup via software. The robust controllers consider a value of $\eta = 2$ to calculate the gains. Moreover a value of $c_x = 90$ is considered for the STA-based controller and $k_\sigma = 5$ for the CSTA.

The considered road profile has the same structure as the one considered in the simulation section. However, due to the physical restrictions of the experimental prototype, such a profile has been scaled down by a factor of 10. Note that, since the physical dimensions of the prototype are fairly different from a real world platform, these changes allows to consider a better example in terms of maximal allowable displacements with a profile that is design to represent somewhat common situations.

As it was the case in the simulation study, the STA-based controller along with the CSTA and the LDO from [25] are considered. Note that, in the physical implementation it is always reasonable to assume that some parameter uncertainty is present on the system and thus, no intentional parameter uncertainty is considered.

Fig. 8 shows the response of the sprung mass position. In this figure, the proposed controllers show a better precision than the LDO. Note that the behavior of the CSTA and the STA are very similar, this is mainly due to the similar robustness properties of the algorithms.

Fig. 9 shows the response for x_3. Notice that a similar response is achieved by all of the controllers. In this figure it is shown that the continuous sliding-mode controllers achieve a better response for x_1 while maintaining a similar response for the unsprung mass.

Fig. 10 shows the control signals. In such a figure, it is possible to see that the response of the continuous sliding-mode controllers do not present a high level of oscillations. In fact, it is possible to see that these controllers require a smaller overall value for the control input to achieve the control objective.

Fig. 11 shows the response of the filtered acceleration $\dot{x}_2$. All of the responses are very similar. This implies a similar level of ride control. However, as can be seen in Fig. 8, the continuous sliding-mode controllers are able to achieve the stabilization of the system in a much more precise manner than the LDO without affecting the ride comfort ina significant way. see Table 1.

In order to provide some quantitative measure for the results, the average of the absolute values of x_1, $\dot{x}_2$, x_3 and u are considered as performance indexes. The value for $|x_1|$ was chosen to assert the precision of the controllers, $|\dot{x}_2|$ gives an indication of ride comfort i.e., for a higher value of $\dot{x}_2$ the ride comfort is compromised; and $|u|$ shows the control activity.
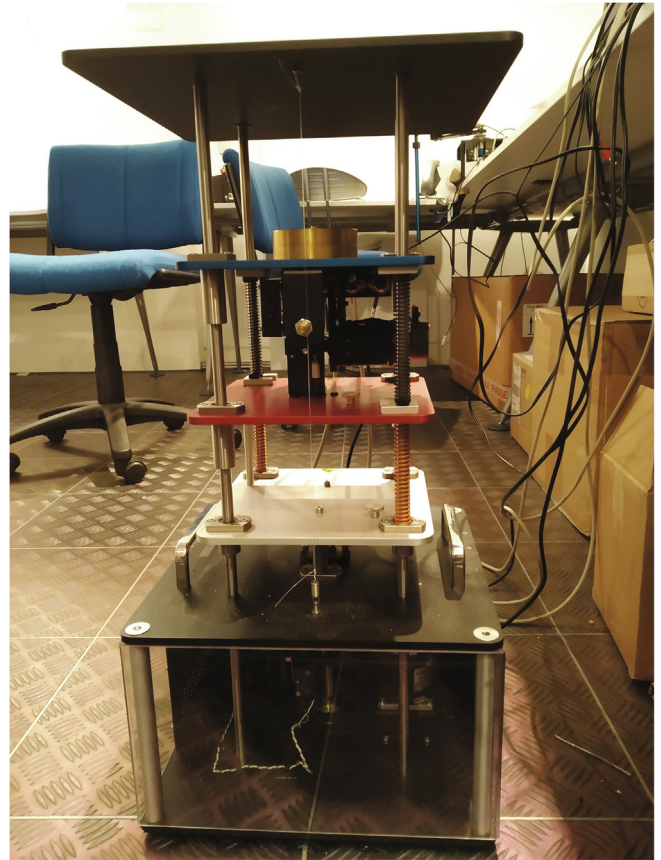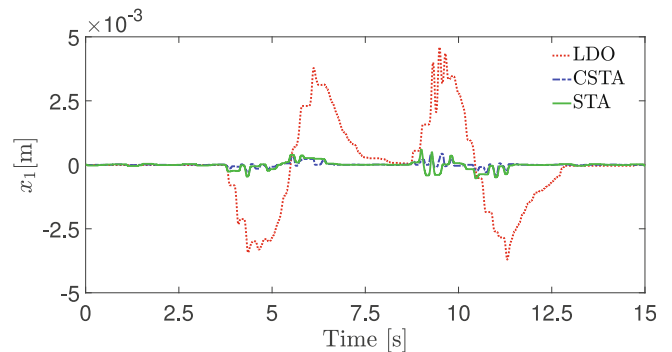
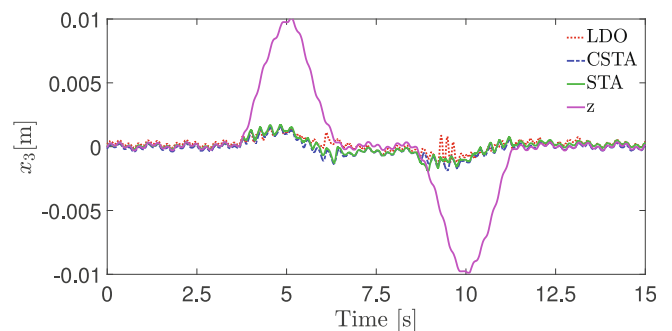**Fig. 7.** Experimental platform.

Fig. 8. Sprung mass position.

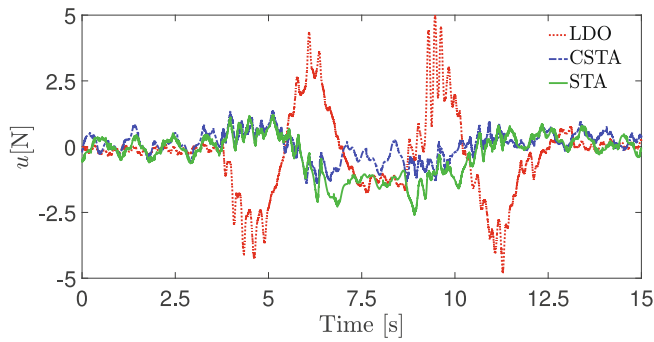

Fig. 9. Unsprung mass position.

Fig. 10. Control signal.
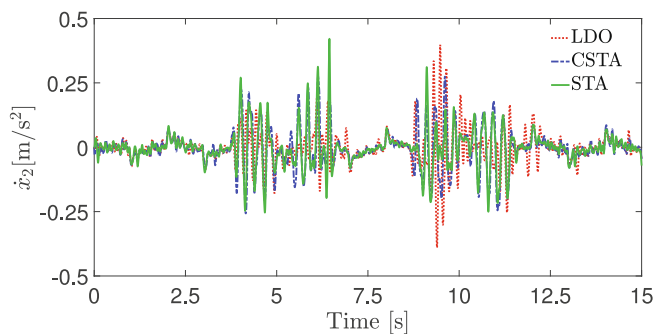
Fig. 11. Filtered accelerations.

Table 1
Quantitative experimental results for the Type II system.

	Average of		
	$|x_1|$	$|\dot{x}_2|$	$|u|$
LDO	0.0014	0.0069	173
STA	0.0068	$9 \cdot 10^4$	224
CSTA	$4 \cdot 10^{-4}$	0.0026	169

Table 2
Quantitative experimental results for the Type II system.

	Average of		
	$|x_1|$	$|\dot{x}_2|$	$|u|$
LDO	1.0×10^{-3}	0.041	1.04
STA	8.0×10^{-5}	0.043	0.61
CSTA	4.2×10^{-5}	0.048	0.41

Table 2 gives the results for the quantitative analysis. In such a table, a better response in terms of precision and control activity can be seen for the CSTA, while the LDO provides a slightly better ride quality. The STA seems to provide a response in the middle, with a slight disadvantage in terms of control activity and precision with respect to the CSTA but an improved ride comfort.

7. Conclusion

In this paper, two different robust control methodologies for the stabilization of an active suspension system were shown. At least exponential stability of the sprung mass was proven in the presence of possibly non-vanishing perturbations. The proposed methodology allows the application of five different robust controllers. The closed-loop stability of the schemes was proven by Lyapunov methods and ISS properties, yielding stronger conclusions to similar schemes in the literature. Some simulations and experimental results show the benefits of the proposed controllers in contrast to classical linear schemes.

Declaration of Competing Interest

The authors declare that they have no known competing financial interests or personal relationships that could have appeared to influence the work reported in this paper.

Acknowledgment

References

[1] N. Tork, A. Amirkhani, S.B. Shokouhi, An adaptive modified neural lateral-longitudinal control system for path following of autonomous vehicles, Eng. Sci. Technol. Int. J. 24 (1) (2021) 126–137.

[2] S. Saha, S.M. Amrr, Design of slip-based traction control system for EV and validation using co-simulation between adams and matlab/simulink, Simulation 96 (6) (2020) 537–549.

[3] H. Sahin, O. Akalin, Articulated vehicle lateral stability management via active rear-wheel steering of tractor using fuzzy logic and model predictive control, SAE Int. J. Commercial Veh. 13 (02-13-02-0008) (2020) 115–128.

[4] R. Kumar, A. Kumar, et al., Nature based self-learning mechanism and simulation of automatic control smart hybrid antilock braking system, Wireless Pers. Commun. 116 (4) (2021) 3291–3308.

[5] C. Kavitha, S.A. Shankar, B. Ashok, S.D. Ashok, H. Ahmed, M.U. Kaisan, Adaptive suspension strategy for a double wishbone suspension through camber and toe optimization, Eng. Sci. Technol. Int. J. 21 (1) (2018) 149–158.

[6] C. Kavitha, S.A. Shankar, K. Karthika, B. Ashok, S.D. Ashok, Active camber and toe control strategy for the double wishbone suspension system, J. King Saud Univ.-Eng. Sci. 31 (4) (2019) 375–384.

[7] M.Ö. Yatak, F. Şahin, Ride comfort-road holding trade-off improvement of full vehicle active suspension system by interval type-2 fuzzy control, Eng. Sci. Technol. Int. J. 24 (1) (2021) 259–270.

[8] T. Yang, N. Sun, Y. Fang, Adaptive fuzzy control for a class of MIMO underactuated systems with plant uncertainties and actuator deadzones: design and experiments, IEEE Trans. Cybern. (2021) 1–14, https://doi.org/10.1109/TCYB.2021.3050475.

[9] T. Yang, N. Sun, Y. Fang, X. Xin, H. Chen, New adaptive control methods for n-link robot manipulators with online gravity compensation: design and experiments, IEEE Trans. Industr. Electron. (2021) 1, https://doi.org/10.1109/TIE.2021.3050371.

[10] Y. Shtessel, C. Edwards, L. Fridman, A. Levant, Conventional sliding mode observers, in: Sliding Mode Control and Observation, Springer, 2014, pp. 105–141.

[11] V.I. Utkin, Sliding modes in control and optimization, Springer Science & Business Media, 1992.

[12] J.A. Moreno, Discontinuous integral control for systems with relative degree two, in: New Perspectives and Applications of Modern Control Theory, Springer, 2018, pp. 187–218..

[13] V. Torres-González, T. Sanchez, L.M. Fridman, J.A. Moreno, Design of continuous twisting algorithm, Automatica 80 (2017) 119–126.

[14] S. Kamal, J.A. Moreno, A. Chalanga, B. Bandyopadhyay, L.M. Fridman, Continuous terminal sliding-mode controller, Automatica 69 (2016) 308–314.

[15] H. Ahmed, H. Ríos, Experimental study of robust output-based continuous sliding-modes controllers for Van der Pol oscillator, IET Control Theory Appl. 12 (15) (2018) 2088–2097.

[16] A.J. Qazi, C.W. de Silva, A. Khan, M.T. Khan, Performance analysis of a semiactive suspension system with particle swarm optimization and fuzzy logic control, Scientific World J. (2014).

[17] K. Rajeswari, P. Lakshmi, PSO optimized fuzzy logic controller for active suspension system, in: 2010 International Conference on Advances in Recent Technologies in Communication and Computing, IEEE, 2010, pp. 278–283.

[18] R. Kothandaraman, L. Satyanarayana, L. Ponnusamy, Grey fuzzy sliding mode controller for vehicle suspension system, J. Control Eng. Appl. Inf. 17 (3) (2015) 12–19.

[19] S. Qamar, T. Khan, L. Khan, Adaptive neuro-fuzzy sliding mode control based strategy for active suspension control, in: 2012 10th International Conference on Frontiers of Information Technology, IEEE, 2012, pp. 107–115.

[20] Ş. Yildirim, Vibration control of suspension systems using a proposed neural network, J. Sound Vib. 277 (4–5) (2004) 1059–1069.

[21] E. Abdellahi, D. Mehdi, M. M'Saad, Active suspension system by h2 and hinfinity: a weights choice procedure for vehicle performance, IFAC Proc. Vol. 33 (14) (2000) 231–235.

[22] J.O. Pedro, M. Dangor, O.A. Dahunsi, M.M. Ali, Intelligent feedback linearization control of nonlinear electrohydraulic suspension systems using particle swarm optimization, Appl. Soft Comput. 24 (2014) 50–62.

[23] V.S. Deshpande, M. Bhaskara, S.B. Phadke, Sliding mode control of active suspension systems using a disturbance observer, in: 2012 12th International Workshop on Variable Structure Systems, 2012, pp. 70–75.

[24] H.I. Basturk, A backstepping approach for an active suspension system, in: 2016 American Control Conference (ACC), IEEE, 2016, pp. 7579–7584..

[25] U.S. Pusadkar, S.D. Chaudhari, P. Shendge, S. Phadke, Linear disturbance observer based sliding mode control for active suspension systems with non-ideal actuator, J. Sound Vib. 442 (2019) 428–444.

[26] V.S. Deshpande, P.D. Shendge, S.B. Phadke, Nonlinear control for dual objective active suspension systems, IEEE Trans. Intell. Transp. Syst. 18 (3) (2017) 656–665.

[27] Y. Pan, P. Du, H. Xue, H.-K. Lam, Singularity-free fixed-time fuzzy control for robotic systems with user-defined performance, IEEE Trans. Fuzzy Syst. (2020) 1, https://doi.org/10.1109/TFUZZ.2020.2999746.

[28] H. Liang, G. Liu, T. Huang, H.-K. Lam, B. Wang, Cooperative fault-tolerant control for networks of stochastic nonlinear systems with nondifferential saturation nonlinearity, IEEE Trans. Syst. Man Cybern.: Syst. (2020) 1–11, https://doi.org/10.1109/TSMC.2020.3020188.

[29] J. Fei, H. Wang, Y. Fang, Novel neural network fractional-order sliding-mode control with application to active power filter, IEEE Trans. Syst. Man Cybern.: Syst. (2021) 1–11, https://doi.org/10.1109/TSMC.2021.3071360.

[30] J. Fei, Z. Wang, X. Liang, Z. Feng, Y. Xue, Fractional sliding mode control for micro gyroscope based on multilayer recurrent fuzzy neural network, IEEE Trans. Fuzzy Syst. (2021) 1, https://doi.org/10.1109/TFUZZ.2021.3064704.

[31] J. Fei, Y. Chen, L. Liu, Y. Fang, Fuzzy multiple hidden layer recurrent neural control of nonlinear system using terminal sliding-mode controller, IEEE Trans. Cybern. (2021) 1–16, https://doi.org/10.1109/TCYB.2021.3052234.

[32] H.K. Khalil, Nonlinear control, Pearson New York, 2015.

[33] A. Polyakov, Nonlinear feedback design for fixed-time stabilization of linear control systems, IEEE Trans. Autom. Control 57 (8) (2012) 2106–2110.

[34] E. Bernuau, A. Polyakov, D. Efimov, W. Perruquetti, Verification of ISS, iISS and IOSS properties applying weighted homogeneity, Syst. Control Lett. 62 (12) (2013) 1159–1167.

[35] A. Levant, Sliding order and sliding accuracy in sliding mode control, Int. J. Control 58 (6) (1993) 1247–1263.

[36] L. Fridman, J. Moreno, R. Iriarte, Sliding modes after the first decade of the 21st century, Lecture Notes Control Inf. Sci. 412..

[37] R. Seeber, M. Horn, Stability proof for a well-established super-twisting parameter setting, Automatica 84 (2017) 241–243.

[38] L. Fridman, J.A. Moreno, B. Bandyopadhyay, S. Kamal, A. Chalanga, Continuous nested algorithms: the fifth generation of sliding mode controllers, in: Recent Advances in Sliding Modes: From Control to Intelligent Mechatronics, Springer, 2015, pp. 5–35.

[39] U. Perez-Ventura, L. Fridman, When is it reasonable to implement the discontinuous sliding-mode controllers instead of the continuous ones? frequency domain criteria, Int. J. Robust Nonlinear Control 29 (3) (2019) 810–828.

[40] L. Zuo, S. Nayfeh, Low order continuous-time filters for approximation of the ISO 2631–1 human vibration sensitivity weightings, J. Sound Vib. 265 (2003) 459–465.